Article

Understanding catalytic synergy in dinuclear polymerization catalysts for sustainable polymers

Francesca Fiorentini[1], Wilfred T. Diment [1], Arron C. Deacy[1], Ryan W. F. Kerr [1], Stephen Faulkner[1] & Charlotte K. Williams [1] ✉

Understanding the chemistry underpinning intermetallic synergy and the discovery of generally applicable structure-performances relationships are major challenges in catalysis. Additionally, high-performance catalysts using earth-abundant, non-toxic and inexpensive elements must be prioritised. Here, a series of heterodinuclear catalysts of the form Co(III)M(I/II), where M(I/II) = Na(I), K(I), Ca(II), Sr(II), Ba(II) are evaluated for three different polymerizations, by assessment of rate constants, turn over frequencies, polymer selectivity and control. This allows for comparisons of performances both within and between catalysts containing Group I and II metals for CO_2/propene oxide ring-opening copolymerization (ROCOP), propene oxide/phthalic anhydride ROCOP and lactide ring-opening polymerization (ROP). The data reveal new structure-performance correlations that apply across all the different polymerizations: catalysts featuring s-block metals of lower Lewis acidity show higher rates and selectivity. The epoxide/heterocumulene ROCOPs both show exponential activity increases (vs. Lewis acidity, measured by the pK_a of $[M(OH_2)_m]^{n+}$), whilst the lactide ROP activity and CO_2/epoxide selectivity show linear increases. Such clear structure-activity/selectivity correlations are very unusual, yet are fully rationalised by the polymerization mechanisms and the chemistry of the catalytic intermediates. The general applicability across three different polymerizations is significant for future exploitation of catalytic synergy and provides a framework to improve other catalysts.

Earth abundant element catalysis is essential to meet UN Sustainable Development Goals, and s-block metals are particularly attractive due to their abundance, low toxicity, diamagnetism, lack of redox chemistry and lack of color[1-6]. Catalytic synergy where two or more metals beneficially interact to enhance rates, selectivity and/or control is a useful strategy to improve their performances[6,7]. Synergic Group I and II metal catalysts have good precedent in homogeneous C-H activation, Grignard, hydro-elementation, Wittig and addition reactions, and as promoters in heterogeneous catalysis, e.g. nitrogen activation[1-5,8-10].

There are also a range of highly effective s-block metal and synergic polymerization catalysts[6,7,11-21]. Doi and Tonks, and co-workers, independently investigated olefin polymerization catalysts where alkali-metal cations coordinated adjacent to the transition metal active site enhanced performances[12,13]. Waymouth, Hedrick and co-workers discovered s-block thioureas that showed very high rates and excellent control in cyclic ester ring-opening polymerizations (ROP)[14,15]. Other Group I and/or II metal catalysts for lactide ROP have shown good rates and, in some cases, stereoselectivity[6,11,18-20]. Satoh and co-workers

[1]Department of Chemistry, University of Oxford, OX1 3TA Oxford, United Kingdom. ✉e-mail: charlotte.williams@chem.ox.ac.uk

showed that simple Group I carboxylates were effective catalysts for anhydride/epoxide ring-opening copolymerization (ROCOP) and switchable polymerizations[16,17].

Here, controlled polymerization catalysts are applied to make sustainable polyesters and polycarbonates. The resulting materials are useful plastics, elastomers, adhesives, fibers and surfactants[22–26]. Future sustainability is addressed by using monomers that are, or could be, derived from biomass, e.g. lactide (carbohydrate), phthalic anhydride (carbohydrate) and propene oxide (glycerol) and/or using waste CO_2[27,28]. All monomers are also existing commercial products, manufactured globally and already used in polymer manufacturing; hence the resulting polymers show real potential for large-scale applications. Polymerizations are atom-economical and products have end-life options including (mechanical) recycling, chemical recycling to monomer and, in some cases, biodegradation[22,23,29]. Three controlled and catalyzed polymerizations are widely applied to produce these polymers: *rac*-lactide (LA) ring-opening polymerization (ROP); phthalic anhydride (PA)/propene oxide (PO) ring-opening copolymerization (ROCOP); and CO_2/PO ring-opening copolymerization (ROCOP) (Fig. 1a, b)[22,25]. This work focusses on dinuclear catalysts which show strong precedent for high rates and selectivity in each of the processes[7,30–44]. Each polymerization operates by a mechanism involving metal alkoxide intermediates and although many (hundreds) of different catalysts are already reported for each separate polymerization, only a few are active for all three processes[25,34,45–48]. To accelerate future catalyst discovery, it would be very useful to identify general catalyst design rules transferable between different polymerizations, to understand structure-property relationships and to better exploit catalytic synergy.

Pioneering work from the groups of Coates, Nozaki and Lu, amongst others, demonstrated the significant potential of homodinuclear CO_2/epoxide ROCOP catalysts, mechanistic hypotheses proposed that two metals at optimum distances significantly enhance rates[34–36,41]. We, and others, reported heterodinuclear metal catalysts, some of which showed better performances than homodinuclear analogs[37,38,49–53]. However, only certain metal combinations were synergic[7,54]. Understanding structure-property relationships is very demanding and in many other cases there was no correlation between activity and any measurable catalyst structural parameter[38,52,53,55]. For example, the activities of a series of CO_2/epoxide ROCOP Mg(II)M(II) catalysts (M(II) = first row transition metals, Mg(II)) showed no correlation with trends in metallic ionic radii, bond dissociation energies, water exchange constants, electronegativity or oxophilicity[52]. Mashima and co-workers showed no correlation between the activities, for CO_2/epoxide ROCOP, of a series of tetranuclear Zn(II)Ln(III)$_3$ catalysts (Ln = lanthanide series) and trends in ionic radii, ligand exchange rates or bond dissociation energies[38]. In epoxide/anhydride ROCOP, synergic Al(III)M(I) catalysts were most active when M(I) = K(I), but the rationale for this metal partnership was not obvious[44]. In LA ROP, s-block metal catalysts often showed the highest rates when using Na(I) or K(I)[6,14–16,18,19,56–58]. Nonetheless, comparisons between Group I metal catalysts revealed contrasting trends: some authors proposed activity increased with ionic radius, whilst others hypothesized the exact opposite to rationalize experimental data[6,14–16,18,19,56–58].

Results

Recently, we reported the first heterodinuclear Co(III)K(I) catalysts for PO/CO_2 ROCOP (Fig. 1c)[50]. Detailed kinetic and DFT analyses implicated a 'dinuclear metallate' mechanism featuring an anionic Co(III) and cationic K(I) catalyst and with a rate determining step involving epoxide ring opening by the carbonate nucleophile coordinated to the s-block metal (Supplementary Fig. 1)[51]. Here, two systematic series of Co(III)M(I/II) catalysts, where M(I/II) = Group I (Na(I), K(I), Rb(I), Cs(I)) or Group II (Ca(II), Sr(II), Ba(II)) are compared for PO/CO_2 ROCOP, PO/PA ROCOP, and *rac*-LA ROP, to investigate whether any general structure-performance relationships exist.

The series of catalysts were synthesized using a common route which involved reacting the dialdehyde precursor, Co(OAc)$_2$, and the Group I/II metal acetate, followed by the addition of ethylene diamine to form the Co(II)M(I/II) complexes, which were oxidized to the Co(III)M(I/II) catalysts with acetic acid, in air (Fig. 2)[50]. The catalysts were purified and isolated as brown powders in good yields (51–74%). The spectroscopic data (^1H, $^{13}C\{^1H\}$, COSY, HSQC, HMBC NMR and IR spectroscopy) are all consistent with the proposed structures, and purity of each complex was confirmed by elemental analysis (Supplementary Figs. 2–20)[8,50]. The complexes were also analyzed by single crystal X-ray diffraction which confirmed the heterodinuclear complexation and revealed 'cobaltate' structures, where the phenolate and acetate ligands are anionic donors (X-type) to the Co(III) center (Fig. 3, Supplementary Figs. S21 and S23)[51]. For the Co(III)M(II) series there are two bridging acetate ligands and one coordinated only to the M(II) center. All the complexes have intermetallic separations ~ 3–4 Å, a distance relevant to other dinuclear catalysts[21,36,49]. The solid-state structures highlight the different coordination chemistries between the s-block metals and the ligand. s-Block metals with smaller radii, like Ca(II) and Na(I), distort the ligand to minimize bond lengths, whilst larger cations, e.g. Rb(I), coordinate above the ligand-Co(III) plane and dimerize in the solid state. Metals in the medium size range, e.g. Sr(II), Ba(II), and K(I), coordinate within the ligand plane (Fig. 3, Supplementary Figs. S21–S27). The formation of cobaltate complexes is significant since
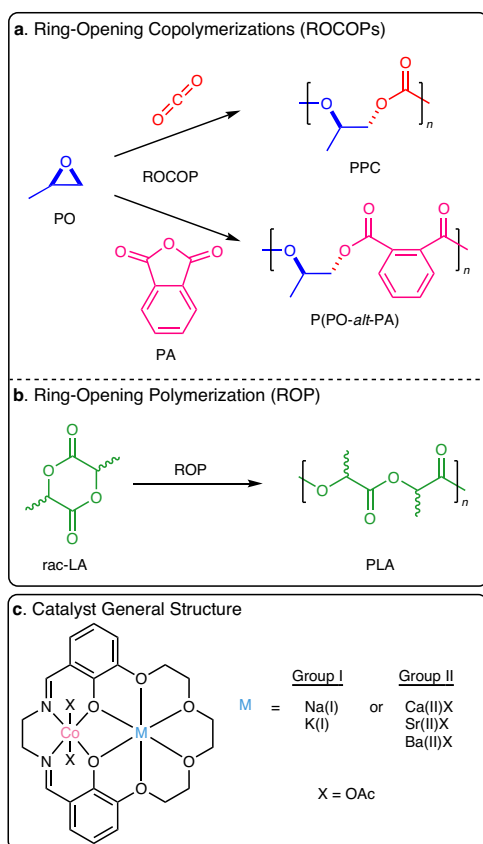

Fig. 1 | The three polymerizations and the catalyst structures investigated. **a** Scheme illustrating ring-opening copolymerization (ROCOP) of propene oxide (PO) and CO_2 to form poly(propene carbonate) (PPC); ROCOP of PO and phthalic anhydride (PA) to form or poly(PO-*alt*-PA). **b** Illustration of ring-opening polymerization (ROP) of *rac*-lactide (*rac*-LA) to form poly(lactide) (PLA); **c** Catalysts reported in this work (see Supplementary Information for details).
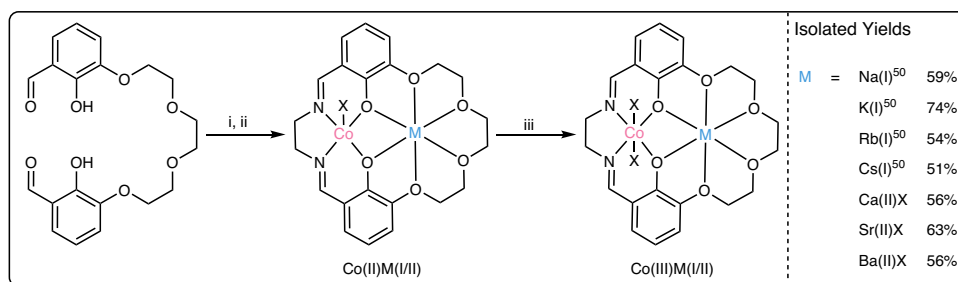
Fig. 2 | Catalyst Synthesis. Co(III)M(I/II) catalysts, M(I/III) = Na(I), K(I), Rb(I), Cs(I), Ca(II), Sr(II), Ba(II), with isolated yields (see supplementary information for experimental details). Reagents: i) Co(OAc)$_2$, M(I)(OAc) or M(II)(OAc)$_2$, MeCN, 1 h; ii) ethylene diamine, MeCN, 16 h; iii) Acetic acid, MeCN, air, 72 h[50].
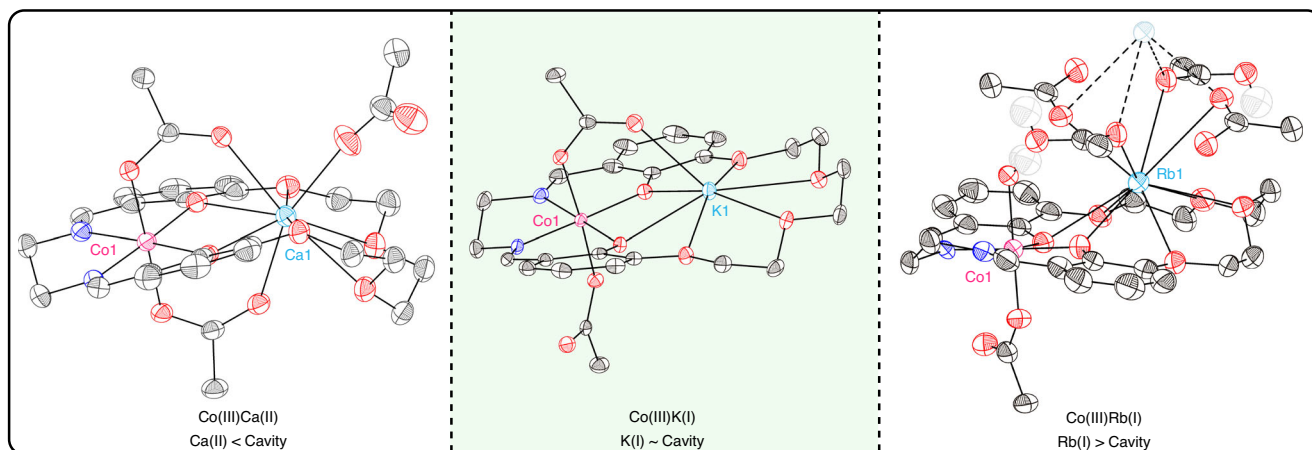

Fig. 3 | Molecular structures of Co(III)Ca(II) (LHS), Co(III)K(I) (middle), and Co(III)Rb(I) (RHS) determined by X-ray diffraction (Supplementary Figs. 21–25). The structures illustrate the structural differences between small, medium and large s-block metals and coordination to the ligand. Selected hydrogen atoms are omitted for clarity. Thermal ellipsoids are represented at 40% probability. Black spheres represent carbon atoms, red represent oxygen, dark blue represent nitrogen and pale gray represent hydrogen.

Table 1 | Data for propene oxide (PO)/CO$_2$ ROCOP using the Co(III)M(I/II) catalysts, where PPC is poly(propene carbonate) and PC is propene carbonate

Entry	Catalyst	Time/h	Productivity TON[a]	Activity TOF/h^{-1}[b]	Rate coefficient k_{obs}/ ×10^{-3} s^{-1}[c]	Selectivity CO$_2$/%[d]	Selectivity PPC/%[e]	PPC M_n [Đ]/ g mol^{-1}[f]
1	Co(III)Ca(II)	22	194 ± 10	5 ± 1	0.36 ± 0.02	93	38 ± 4	700 [1.17]
2	Co(III)Sr(II)	23	889 ± 44	23 ± 2	1.79 ± 0.14	97	50 ± 5	2100 [1.07]
3	Co(III)Ba(II)	21	856 ± 43	30 ± 2	2.36 ± 0.17	97	61 ± 6	2500 [1.11]
4[50]	Co(III)Na(I)	5	600 ± 30	104 ± 8	7.52 ± 0.60	>99	79 ± 2	2300 [1.08]
5[50]	Co(III)K(I)	4	1360 ± 68	528 ± 42	38.20 ± 3.06	>99	98 ± 2	5900 [1.10]
6[50]	Co(III)Rb(I)	23	1240 ± 62	88 ± 7	6.37 ± 0.51	>99	91 ± 3	6500 [1.07]
7[50]	Co(III)Cs(I)	23	1080 ± 54	88 ± 7	6.34 ± 0.51	>99	84 ± 3	5600 [1.08]

Reaction conditions: catalyst (0.025 mol%, 3.6 mM), PO (5 mL, 14.3 M), 1,2-cyclohexane diol (0.5 mol%, 71 mM), 20 bar CO$_2$, 50 °C.
[a]Turnover number (TON) = moles PO consumed/moles catalyst. PO conversion determined from ^{1}H NMR spectra integrals for PPC (4.92 ppm), PC (4.77 ppm) and PPO (3.46-3.64 ppm), using mesitylene as an internal standard (0.05 mol%, 36 mM).
[b]Turnover frequency (TOF) are determined from 5 to 20% conversions, in all cases (Supplementary Tables 1 and 2, Supplementary Eq. (1)).
[c]Calculated from linear ln([PO]$_t$/[PO]$_0$) vs. time plots (Supplementary Figs. 28 and 30).
[d]Selectivity for CO$_2$ conversion, determined from PO conversion to PPC + PC/overall PO conversion (using NMR integrals).
[e]Selectivity for PPC formation, determined as PO conversion to PPC/overall PO conversion (using ^{1}H NMR spectroscopy integrals).
[f]Determined by GPC, in THF, at 30 °C, using narrow MW polystyrene calibrants.

DFT investigations implicated this structure is present in the active site during catalysis[50,51].

All the new catalysts were tested for PO/CO$_2$ ROCOP under common conditions: in neat epoxide using 1:4000, [catalyst]:[PO]$_0$ (0.025 mol% catalyst), at 20 bar CO$_2$, 50 °C and with 20 equivalents vs. catalyst of 1,2-cyclohexane diol (CHD, 0.5 mol%) (Table 1). These conditions are selected to allow comparisons against some of the best performing catalysts in the field and represent 'demanding' loadings[50,51]. The diol, CHD, controls the polycarbonate molar mass and dispersity; it is used here to target polyols with M_n < 6000 g/mol which are relevant to polyurethane, surfactant and resin applications[24]. Catalysts often show reduced rates when using excess diol, therefore identification of high activity synergic catalysts is important[50,59,60].

All catalysts were active but there are clear differences with turnover frequencies (TOFs) ranging from 5 to 588 h^{-1} depending on the metal combination. For all complexes, the catalytic rates are determined per mole of complex since DFT investigations indicated that

Table 2 | Data for propene oxide (PO)/phthalic anhydride (PA) ROCOP with Co(III)M(I/II) catalysts

Entry	Catalyst	Time/h	Productivity TON[a]	Activity TOF/h[-1b]	Rate coefficient k_{obs}/×10^{-6} M^{-1} s^{-1c}	Selectivity polyester/%[d]	Polyester M_n [Đ]/g mol^{-1e}
1	Co(III)Ca(II)	21	88 ± 2	4 ± 2	17.4 ± 7.4	>99	4600 [1.13] 11600 [1.02]
2	Co(III)Sr(II)	30	87 ± 1	3 ± 1	10.5 ± 3.2	>99	5100 [1.08]
3	Co(III)Ba(II)	30	84 ± 1	3 ± 1	11.2 ± 3.6	>99	6000 [1.11]
4	Co(III)Na(I)	7	88 ± 2	12 ± 1	45.8 ± 1.6	>99	4200 [1.12]
5	Co(III)K(I)	3	89 ± 1	31 ± 1	122.7 ± 4.2	>99	4500 [1.11]

Reaction conditions: Catalyst (0.1 mol%, 0.0143 mM), PA (10 mol%, 1.43 mM), PO (1 mL, 14.3 M), 50 °C (Catalyst:PA:PO, 1:100:1000).
[a]TON determined by ^{1}H NMR spectroscopy using integrals for PA (8.10–7.85 ppm) and P(PO-alt-PA) (7.75–7.40 ppm).
[b]Turnover frequency (TOF) is reported from gradients of conversion vs. time plots, from 5 to 20% conversions, in all cases (Supplementary Tables 3 and 4, Supplementary Eq. (2)).
[c]Rate coefficient is the gradient of linear fits to plots of [PA]t vs. time (Supplementary Fig. 36).
[d]Selectivity for polyester determined by ^{1}H NMR spectroscopy using integrals for P(PO-alt-PA) and any PPO (3.46–3.64 ppm).
[e]Determined by GPC, in THF, at 30 °C, using narrow dispersity polystyrene calibrants.

only one acetate group initiates polymerization[51]. The catalysts also showed variable selectivity for polycarbonate vs. cyclic carbonate formation, with values between 38 and 98% (Table 1). In all cases, the uptake of CO_2 was very high, from 93 to 99%, resulting in the formation of highly alternating polycarbonates. All the polycarbonates showed narrow, monomodal molar mass distributions (Đ ≤ 1.17); these features signal controlled polymerization catalysis (Supplementary Figs. 31 and 33)[22,29]. Generally, the catalysts featuring Group I metals, M(I), were more active and selective than those with Group II metals, M(II). It is immediately clear that catalyst performance rationale by 's-block metal ion size' are inappropriate since Co(III)K(I) shows the best activity and selectivity, yet Co(III)Ba(II) or Co(III)Sr(II) feature cations of similar sizes and stronger ligand binding affinities yet are significantly worse catalysts (Supplementary Figs. 34 and 35)[61].

Epoxide/anhydride ROCOP is an attractive route to polyesters with variable structures and properties, due to the wide range of polymerizable monomers, many of which are commercial products and/or bio-based[29,62]. It yields semi-aromatic, rigid, aliphatic and/or functionalised polyesters and, in contrast to cyclic ester ROP, shows favorable thermodynamics, allowing high yields of polyesters[29,62]. Given its utility, better understanding of catalyst design parameters are urgently needed. The Co(III)M(I/II) catalysts were evaluated using commercial, and widely used, monomers; PO and PA. Polymerizations were conducted in neat PO, using loadings of 1:100:1000 [catalyst]:[PA]$_0$:[PO]$_0$ (i.e. 0.1 mol% catalyst, 10 mol% PA) and at 50 °C (Table 2). Once again, there were clear differences in catalytic activity, with Co(III)K(I) being more active than the Na(I) analog, and both being faster than M(II) catalysts. Plots of P(PO-alt-PA) molar mass against anhydride conversion were linear, and the dispersity values remained narrow throughout the reactions (Supplementary Figs. 37 and 46). These features are all consistent with well-controlled polymerizations and single site catalysts; important factors in any structure-activity relationship investigation. The Co(III)K(I) catalyst was also highly active and selective using a range of other epoxides and anhydrides to produce different polyesters (Supplementary Table 5, Supplementary Figs. 47 and 55).

Polylactide (PLA) is the leading bio-derived polymer used in packaging, fiber and plastics applications[22,26,63]. It has lower greenhouse gas emissions than incumbent fossil-plastics since it is plant-derived, and, after use, PLA is recyclable and/or compostable[22,26,63]. LA ROP is used to produce PLA, and its efficiency depends upon catalyst selection[11]. The catalysts were tested using 1:100:1000 [catalyst]$_0$:[LA]$_0$:[PO]$_0$ (i.e. 0.1 mol% catalyst), at 50 °C. The PO serves as both reaction solvent and initiator, since it reacts with the catalyst to form the true metal-alkoxide 'initiators' (acetate ligands cannot initiate)[25]. When monitoring the reaction only LA ROP occurred; no ether linkages from PO ROP were observed in the PLA.

The most active catalyst was Co(III)K(I), achieving a TOF of 912 h^{-1}, and in all cases the Co(III)M(I) catalysts outperform the Co(III)M(II)

species (Table 3). The catalysts all show good polymerization control, as evidenced by monomodal molar mass distributions and linear plots of molar mass vs. conversion (Supplementary Figs. 61 and 70). The PLA was atactic except for the most active Co(III)K(I) catalyst which showed moderate iso-selectivity (P_i = 0.71, Supplementary Table 8). Comparing the M(I) and M(II) catalysts shows that activity trends do not correlate with the s-block cationic radius. For example, Co(III)K(I) and Co(III)Ba(II) have very similar radii (K(I) = 1.46 Å, Ba(II) = 1.52 Å), yet the K(I) catalyst is 6 times more active than the Ba(II) analog (Table 3; Supplementary Fig. 71)[64].

Discussion

To understand the experimental trends in activity and selectivity data, the polymerization mechanisms should be discussed. As mentioned, comparing M(I) vs. M(II) catalysts reveals that rationale based only on ionic radii are incomplete or inaccurate. There was also no correlation between rates or selectivity and published s-block cation binding affinity to 18-crown-6, or ionic radius data (Supplementary Figs. 34, 35, 69). Thus, our attention turned to evaluating the s-block metal Lewis acidity, since the rate determining step in all three polymerizations involves a metal-oxygenated nucleophile, proposed as coordinated to the s-block metal[19,49–51,54]. Prior work has revealed that metal Lewis acidity can be accurately quantified using the pK_a of the metal aqua complex, in water[65]. Recently, Blakemore and Kumar reported an in-depth investigation of s-block cation Lewis acidity, analyzing metal triflates dissolved in organic solvents by Guttmann Beckett ^{31}P NMR titration methods[65]. In all solvents tested, plots of s-block cation pK_a vs. the change in ^{31}P NMR chemical shift of triphenyl phosphine oxide, used as a titrant, were linear. This confirms that pK_a can be used to quantify Lewis acidity in organic media[65].

In the current series of catalysts, the plot of PO/CO_2 ROCOP activity against s-block metal pK_a value showed exponential increase, i.e. the fastest catalysts featured the least Lewis acidic metals, Na(I) and K(I) (Fig. 4a). The exponential fits were confirmed by linear fits to ln(TOF) vs. ln(pK_a) and ln(k_{obs}) vs. ln(pK_a) plots (Supplementary Figs. 73 and 74). Analysis of the selectivity for polycarbonate (PPC) vs. s-block metal Lewis acidity (pK_a) showed a linear correlation with the most selective catalysts featuring the least Lewis acidic s-block metals, Na(I) and K(I) (Fig. 4c). Such metal Lewis acidity-performance correlations in CO_2/epoxide ROCOP are so far without precedent yet should be very useful for future catalyst design.

Polymerization mechanisms that were previously established using kinetics, DFT and reactivity investigations are used to rationalize the trends[50,51]. The Co(III)M(I) catalysts showed second-order rate laws, dependent upon both catalyst and epoxide concentrations[50,51]. Rates were zeroth order in CO_2 pressure from 10 to 40 bar[50,51]. The 'dinuclear metallate' mechanism involves a rate-determining step where PO is coordinated at Co(III) and is ring-opened by a K(I)-carbonate (Fig. 4e, Supplementary Fig. S1)[50,51]. The selectivity-determining step controls

Table 3 | Data for *rac*-lactide (LA) ring opening polymerization using the Co(III)M(I/II) catalysts

Entry	Catalyst	Time/h	TON[a]	TOF/h^{-1}[b]	k_{obs}/$\times 10^{-3}$ s^{-1}[c]	M_n [Đ] / g mol^{-1}[d]
1	Co(III)Ca(II)	4.5	90	42 ± 4	0.21 ± 0.02	3300 [1.22]
2	Co(III)Sr(II)	1.7	97 ± 1	212 ± 12	1.04 ± 0.06	4700 [1.23]
3	Co(III)Ba(II)	1.7	97 ± 1	147 ± 10	0.72 ± 0.05	5600 [1.61]
4	Co(III)Na(I)	0.2	88 ± 1	670 ± 22	3.29 ± 0.21	4100 [1.30]
5	Co(III)K(I)	0.2	90 ± 4	912 ± 83	4.48 ± 0.41	4800 [1.23]

Reaction conditions: catalyst (0.1 mol%, 14.3 mM), *rac*-LA (10 mol%, 1.43 M), PO (1 mL, 14.3 M), 50 °C ([Catalyst]$_0$:[LA]$_0$:[PO]$_0$, 1:100:1000).
[a]TON determined by ^{1}H NMR spectroscopy from normalized integrals for *rac*-LA (4.99–5.09 ppm, 2 H) and PLA (5.10–5.26 ppm, 2H).
[b]Turnover frequency (TOF) determined from 5 to 70% conversion (Supplementary Tables 6 and 7, Supplementary Eq. (S3)).
[c]Calculated from linear fits to plots of ln([*rac*-LA]$_t$/[*rac*-LA]$_0$) vs. time for Co(III)Na(I) and Co(III)K(I); for Co(III)Ca(II), Co(III)Sr(II) and Co(III)Ba(II) slow initiation was handled using [PLA] = A(1 − exp(−k_{obs}t))
(Supplementary Figs. 56 and 60)[71].
[d]Determined by GPC in THF, at 30 °C, using narrow dispersity polystyrene standards and multiplied by 0.58 as the correction factor[72].

the relative quantities of polycarbonate vs. cyclic carbonate formed. This step is pre-rate determining and equilibrates a Co(III)K(I)-alkoxide (II) with CO_2 to form the Co(III)K(I)-carbonate (III); the equilibrium is controlled by the CO_2 insertion chemistry[50,51]. The by-product, cyclic carbonate, forms only from the alkoxide intermediate and so reducing its relative concentration increases selectivity for polycarbonate.

For the Co(III)M(I/II) catalysts, rates were greater with weakly Lewis acidic s-block metals. It is proposed that reducing the metal Lewis acidity slightly destabilises the metal-carbonate intermediates (i.e. higher ground state energy) and may also reduce transition state energies during epoxide ring-opening. The selectivity for polycarbonate also increases as s-block metal Lewis acidity decreases. By the same rationale, the least acidic s-block metals feature slightly destabilized alkoxide intermediates (i.e. higher ground state energy). DFT calculations suggested that the alkoxide intermediate is stabilized by interaction with an adjacent carbonate group on the growing polymer chain (II, Fig. 4d, e). As the s-block metals' Lewis acidity decreases, this interaction weakens, which further destabilizes the alkoxide intermediate and drives CO_2 insertion to increase the formation of the carbonate intermediate. The Co(III)Rb(I) and Co(III)Cs(I) catalysts do not fit the activity or selectivity trends and were not tested in other polymerizations. These complexes feature cations of sufficiently large ionic radii that it limits effective coordination within the macrocycle, as observed in the solid-state structures, and results in aggregation. These aggregates complicate structure-activity correlations (Rb(I) = 1.56 Å, Cs(I) = 1.71 Å, vs. K = 1.46 Å) (Supplementary Figs. 75 and 76)[50,64].

Analysis of the data and trends for the series of catalysts in PO/PA ROCOP reveals a related activity trend to that observed for PO/CO_2 ROCOP. The activity, as assessed by either rate constant or turnover-frequency, increases exponentially as the Lewis acidity decreases (Fig. 5a). It is very interesting to note that once again the rates increase exponentially vs. metal cation pK_a value (linear plots of ln(TOF) vs. ln(pK_a) and ln(k_{obs}) vs. ln(pK_a), Supplementary Figs. 77 and 78). For these catalysts, the rate law for epoxide/anhydride ROCOP is first order in epoxide and zero-order in anhydride concentration, respectively (Supplementary Figs. 79 and 80)[44,66]. A related Al(III)K(I) catalyst showed a similar rate law and was proposed to operate by a related 'metallate' mechanism by DFT calculations[44]. In this series of catalysts, the proposed rate determining step involves epoxide coordination at Co(III) and ring-opening by M(I)- or M(II)-carboxylate intermediates.

The experimental data show faster rates with less Lewis acidic s-block metals. This data is rationalized by the least Lewis acidic s-block metals having slightly destabilized, and hence more reactive, carboxylate intermediates, compared to those with more Lewis acidic metals. The same exponential increases to activity vs. pK_a data for the two different epoxide/heteroallene ROCOP is fully consistent with the polymerizations having related rate-determining steps. Finally, both polymerizations ROCOPs involve rate determining steps

where nucleophilic attack occurs from bidentate nucleophiles, either carbonate (CO_2/epoxide) or carboxylate (anhydride/epoxide) intermediates. It is tentatively proposed that these complexes may show exponential rate vs. acidity relationships since these key s-block metal intermediates can accommodate both monodentate and bidentate coordination modes, as observed in the solid-state structures. Comparing the two polymerizations, the activities for PO/PA ROCOP are considerably lower than for the equivalent polymerizations using CO_2 likely due to the lower nucleophilicity of the M(I/II) carboxylate vs. carbonate in the rate determining step. Once again 'model' pK_a values help to rationalize the rate differences since formic acid (pK_a = 3.75) is considerably more acidic than carbonic acid (pK_a = 6.37) and weaker acids are shown, in this work, to be more reactive[67].

In the series of catalysts, the rates of LA ROP, as assessed either from rate constants (k_{obs}) or TOFs, increase linearly with decreasing s-block metal Lewis acidity (Fig. 6a). The coordination-insertion mechanism for LA ROP is proposed in common with many other metal-based lactide polymerization catalysts[6,11]. The polymerization kinetics are all first order in lactide and the rate-limiting step is proposed to involve metal-alkoxide intermediate attack at (metal-)coordinated lactide (Fig. 6c, Supplementary Figs. S56 and S57). It is proposed that the lactide coordinates at the Co(III) site and the M(I/II)-alkoxide attacks it – with the metals exhibiting similar roles to those in epoxide/heteroallene ROCOP. The experimental data trends are rationalized since decreasing the s-block Lewis acidity results in a destabilized metal-alkoxide intermediate which shows higher lability in the lactide insertion reaction (and faster rates). The different activity vs. s-block metal Lewis acidity data trends reveal new information to better understand catalyst design parameters: intermediates involving bidentate species, such as carboxylates or carbonates, show exponential increases in activity, whereas those which involve monodentate ligands, such as alkoxides, show linear trends. Accordingly, the PO/CO_2 selectivity and lactide rates show linear correlations and depend upon the reactivity of metal-alkoxide intermediates (Fig. 5d). There was also a linear correlation between the degree of isotacticity, P_i, and s-block metal Lewis acidity consistent with the alkoxide intermediate controlling stereoselectivity (Supplementary Fig. 81).

Overall, the series of Co(III)M(I/II) catalysts show unprecedented but reproducible correlations between both catalytic activity and selectivity (for polymer or stereoselectivity) and the s-block metal Lewis acidity. These correlations apply equivalently between three different polymerizations, which are all relevant to the future increased production of sustainable polyesters and polycarbonates. The findings are significant since they signal clearly the methods to optimize performances and provide improved understanding of the physical-chemical factors responsible for high rates/selectivity. Reducing the Lewis acidity of the s-block metal benefits both the rates and selectivity of these polymerizations, with the Co(III)K(I) catalyst consistently performing best. In the future, research should target ancillary ligand modifications to fine-tune K(I) Lewis acidity, for example by
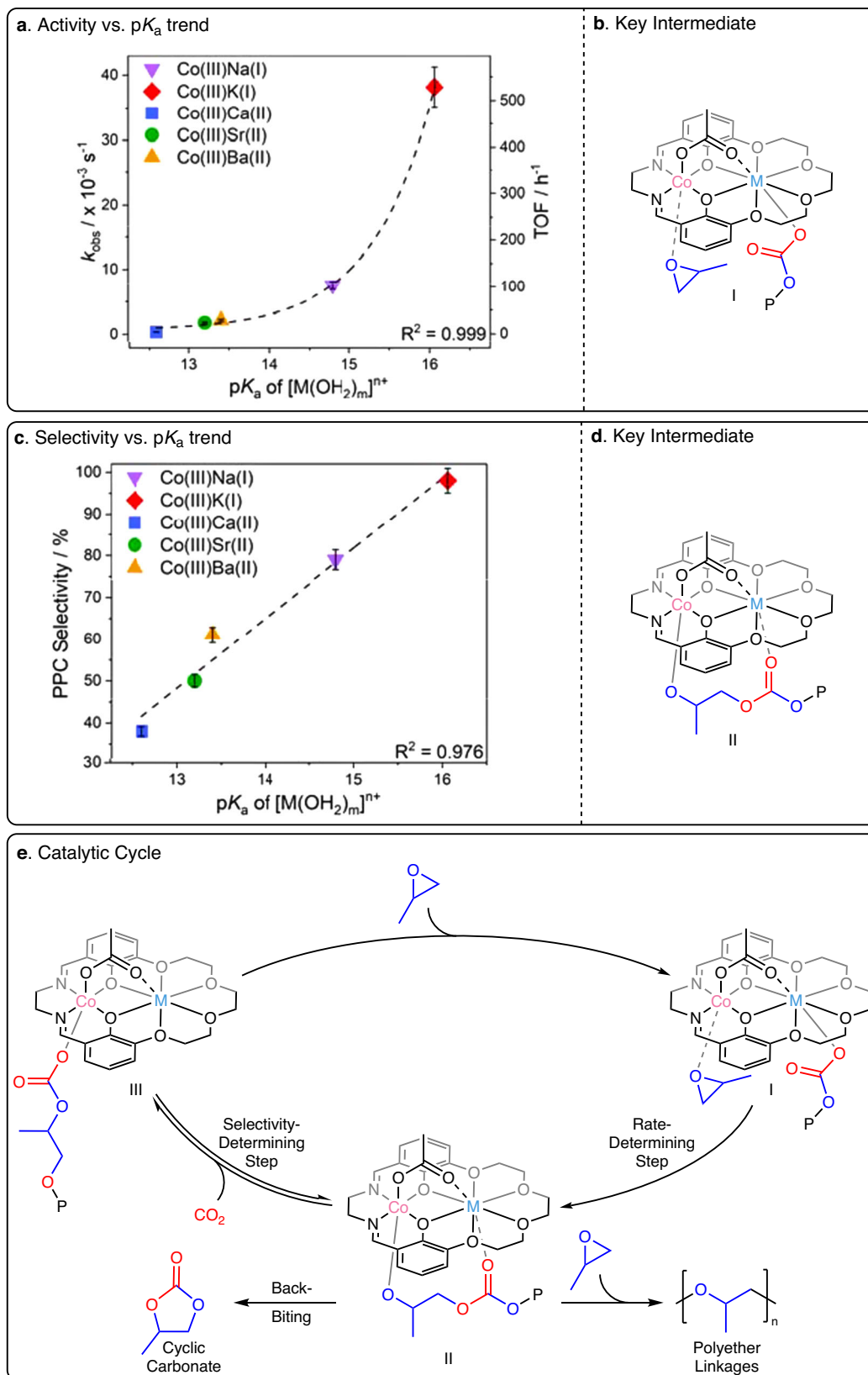
Fig. 4 | Structure-activity and structure-selectivity trends for propene oxide and carbon dioxide ROCOP, with the catalytic cycle. a Plots of k_{obs} and TOF against the pK_a of $[M(OH_2)_m]^{n+}$ for PO/CO_2 ROCOP catalyzed by Co(III)M(I/II); error bars represent the standard error of the mean; **b** Structure of the proposed rate determining intermediate; **c** Plot of selectivity against s-block metal pK_a value; error bars represent the standard error of the mean; **d** Structure of the selectivity determining intermediate; **e** Catalytic cycle for PO/CO_2 ROCOP catalyzed by Co(III) M(I/II) with rate and selectivity determining steps identified. P denotes the polymer chain.
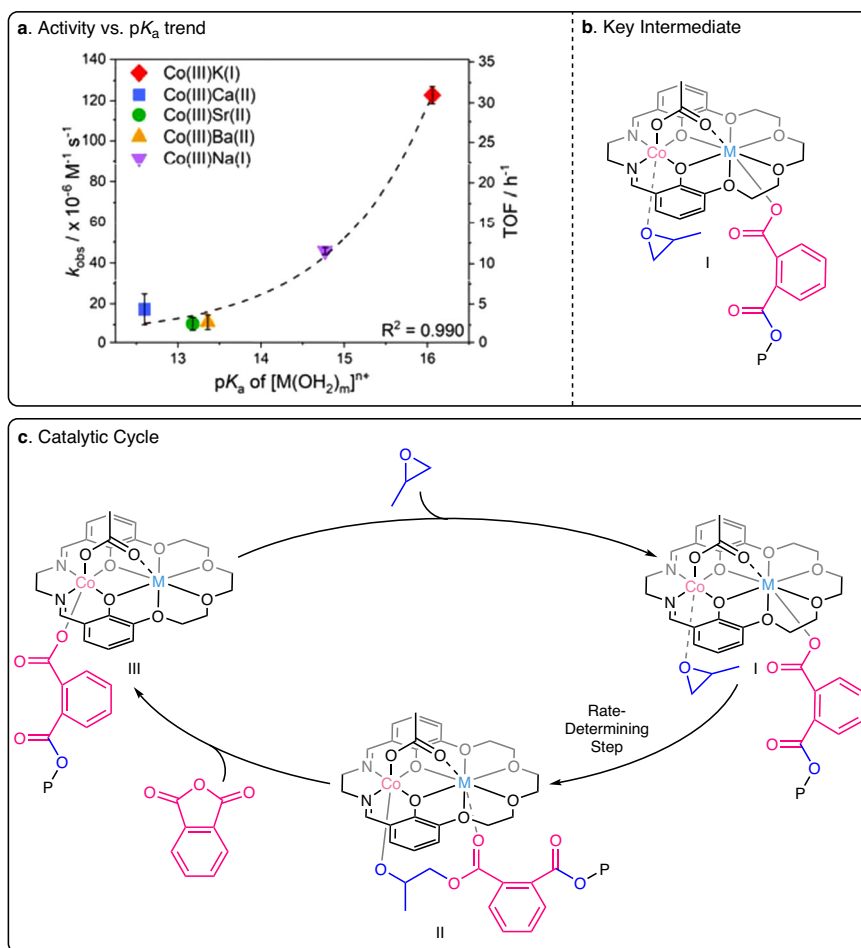
Fig. 5 | Structure-activity trends for propene oxide and phthalic anhydride ROCOP, with the catalytic cycle. a Plot of k_{obs} and TOF against pK_a of the s-block metal for PO/PA ROCOP catalyzed by Co(III)M(I/II); error bars represent the standard error of the mean; **b** Key intermediate that determines activity; **c** Catalytic cycle for PO/PA ROCOP catalyzed by Co(III)M(I/II). P denotes the polymer chain.

altering the substituents adjacent to the 'ether' donors and by investigating different numbers of ether donors. The trends uncovered for these heterodinuclear catalysts should be applicable to other polymerization catalysts including those based on simple s-block metal cations and synergic catalysts with other metals. It is recommended that in future all high-performance s-block metal catalysts are assessed using pK_a as a measure of Lewis acidity and that Group II metals catalysts are routinely compared with Group I analogs[6,18]. In synergic dinuclear catalysis, replacing an expensive second transition metal or even obviating phosphonium co-catalyst by ligand design to incorporate s-block metals should be prioritized as a means to rationally re-design metal Schiff-base and salen catalysts for heteroallene/epoxide ROCOP. The Co(III)K(I) catalysts show excellent rates and selectivity in three different polymerizations and so could be highly effective using monomer mixtures, following rules of switchable catalysis, to produce multi-block polymers and phase-separated materials[25]. The structure-performance relationships uncovered in this work are expected to apply to other synergic s-block metal catalysts for organic transformations, polymerizations and may even shed light on roles played by s-block cation 'promoters' which are very common in heterogeneous catalysis[9,68,69]. There are even di-zinc histone deacetylase enzymes activated by K(I) cations and these Lewis acidity trends may also aid understanding of synergic bio-catalysts[70]. Finally, the activation and utilization of CO_2 is of central importance and the current structure-performance trends should help to reduce both the cost and weight of metals applied and guide mechanistic understanding of CO_2 'insertions' and transformations.

A series of heterodinuclear Co(III)M complexes, where M = Group I or II cations, were compared as polymerization catalysts for three processes relevant to future sustainable polymer production: carbon dioxide/epoxide ring-opening copolymerization, anhydride/epoxide ring-opening copolymerization and *rac*-lactide ring-opening polymerization. Each polymerization data set showed clear structure-activity and structure-selectivity trends where the best catalysts feature the least Lewis acidic s-block metals, i.e. Co(III) and Na(I) or K(I). Importantly, the same activity and selectivity trends vs. cation Lewis acidity applied to all three different polymerizations. Such clear structure-performance correlations are very rare in any polymerization catalysis and are without precedent across these different reactions. The activity and selectivity data show clearly that the s-block metal-oxygenate nucleophiles become more reactive when using less Lewis acidic metals. For s-block metal carbonate or carboxylate intermediates rate data increased exponentially, whilst for s-block metal alkoxide intermediates rate or selectivity data increased linearly. The data and correlations help rationalize the beneficial roles played by s-block metals and the chemistry underpinning catalytic metal synergy; they should accelerate future discovery of higher activity, selectivity and controlled catalysts. These are needed to unlock production of sustainable, bio-based and recyclable polymers. In future, the best catalysts should also be investigated for polymerizations of monomer mixtures (e.g. LA, CO_2, PA and PO), exploiting mechanism switches, to efficiently and selectively produce block and copolymers[25]. Such materials diversify the properties and applications for materials made from biomass and CO_2[25].
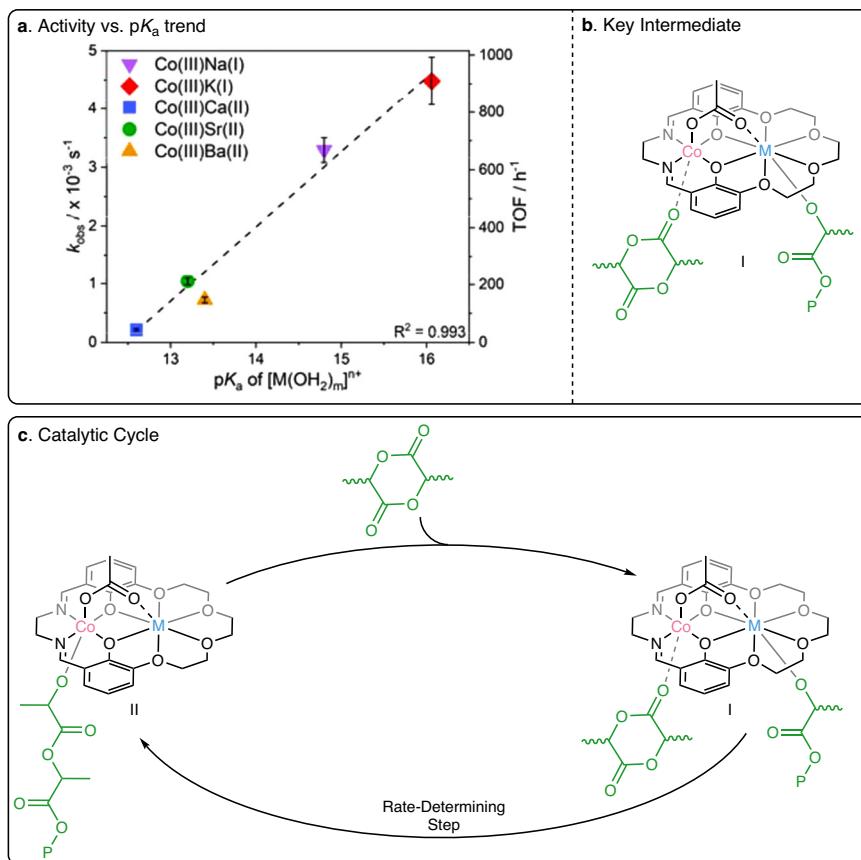
Fig. 6 | Structure-activity trend for racemic lactide ROP, with the catalytic cycle. a Plot of k_{obs} and TOF against pK_a of the s-block metal for *rac*-LA ROP catalyzed by Co(III)M(I/II); error bars represent the standard error of the mean; **b** Proposed structure of the intermediate that determines activity; **c** Catalytic cycle for *rac*-LA ROP catalyzed by Co(III)M(I/II). P denotes the polymer chain.

Data availability

The electronic supplementary information provides data to support the manuscript, all other data are available from the corresponding author. The X-ray crystallographic coordinates for structures reported in this study have been deposited at the Cambridge Crystallographic Data Center (CCDC), under deposition numbers 2250536, 2250537 and 2250538. These data can be obtained free of charge from The Cambridge Crystallographic Data Center via www.ccdc.cam.ac.uk/data_request/cif.

References

1. Bullock, R. M. et al. Using nature's blueprint to expand catalysis with Earth-abundant metals. *Science* **369**, eabc3183 (2020).
2. Bauer, H. et al. Imine hydrogenation with simple alkaline earth metal catalysts. *Nat. Catal.* **1**, 40–47 (2018).
3. Gil-Negrete, J. M. & Hevia, E. Main group bimetallic partnerships for cooperative catalysis. *Chem. Sci.* **12**, 1982–1992 (2021).
4. Magre, M., Szewczyk, M. & Rueping, M. s-Block metal catalysts for the hydroboration of unsaturated bonds. *Chem. Rev.* **122**, 8261–8312 (2022).
5. Gentner, T. X. & Mulvey, R. E. Alkali-metal mediation: diversity of applications in main-group organometallic chemistry. *Angew. Chem. Int. Ed.* **60**, 9247–9262 (2021).
6. Gruszka, W. & Garden, J. A. Advances in heterometallic ring-opening (co)polymerisation catalysis. *Nat. Commun.* **12**, 3252 (2021).
7. Diment, W. T., Lindeboom, W., Fiorentini, F., Deacy, A. C. & Williams, C. K. Synergic heterodinuclear catalysts for the ring-opening copolymerization (ROCOP) of epoxides, carbon dioxide, and anhydrides. *Acc. Chem. Res.* **55**, 1997–2010 (2022).
8. Reath, A. H., Ziller, J. W., Tsay, C., Ryan, A. J. & Yang, J. Y. Redox potential and electronic structure effects of proximal nonredox active cations in cobalt schiff base complexes. *Inorg. Chem.* **56**, 3713–3718 (2017).
9. Chantarojsiri, T., Ziller, J. W. & Yang, J. Y. Incorporation of redox-inactive cations promotes iron catalyzed aerobic C–H oxidation at mild potentials. *Chem. Sci.* **9**, 2567–2574 (2018).
10. Connor, G. P. & Holland, P. L. Coordination chemistry insights into the role of alkali metal promoters in dinitrogen reduction. *Catal. Today* **286**, 21–40 (2017).
11. Fazekas, E. et al. Main group metal polymerisation catalysts. *Chem. Soc. Rev.* **51**, 8793–8814 (2022).
12. Cai, Z., Xiao, D. & Do, L. H. Fine-tuning nickel phenoxyimine olefin polymerization catalysts: performance boosting by alkali cations. *J. Am. Chem. Soc.* **137**, 15501–15510 (2015).
13. Chiu, H.-C., Pearce, A. J., Dunn, P. L., Cramer, C. J. & Tonks, I. A. β-Oxo-δ-diimine nickel complexes: a comparison of tautomeric active species in ethylene polymerization catalysis. *Organometallics* **35**, 2076–2085 (2016).
14. Zhang, X., Jones, G. O., Hedrick, J. L. & Waymouth, R. M. Fast and selective ring-opening polymerizations by alkoxides and thioureas. *Nat. Chem.* **8**, 1047–1053 (2016).
15. Jadrich, C. N. et al. A cation-dependent dual activation motif for anionic ring-opening polymerization of cyclic esters. *J. Am. Chem. Soc.* **144**, 8439–8443 (2022).

16. Saito, T. et al. Alkali metal carboxylate as an efficient and simple catalyst for ring-opening polymerization of cyclic esters. *Macromolecules* **51**, 689–696 (2018).

17. Xia, X. et al. Smart access to sequentially and architecturally controlled block polymers via a simple catalytic polymerization system. *ACS Catal.* **11**, 5999–6009 (2021).

18. Gruszka, W. & Garden, J. A. Salt additives as activity boosters: a simple strategy to access heterometallic cooperativity in lactide polymerisation. *Chem. Commun.* **58**, 1609–1612 (2022).

19. Gruszka, W., Sha, H., Buchard, A. & Garden, J. A. Heterometallic cooperativity in divalent metal ProPhenol catalysts: combining zinc with magnesium or calcium for cyclic ester ring-opening polymerisation. *Catal. Sci. Technol.* **12**, 1070–1079 (2022).

20. Ou, H.-W. et al. Synthesis of sodium complexes supported with nno-tridentate schiff base ligands and their applications in the ring-opening polymerization of l-Lactide. *Inorg. Chem.* **55**, 1423–1432 (2016).

21. Kember, M. R. & Williams, C. K. Efficient magnesium catalysts for the copolymerization of epoxides and CO2; using water to synthesize polycarbonate polyols. *J. Am. Chem. Soc.* **134**, 15676–15679 (2012).

22. Zhang, X., Fevre, M., Jones, G. O. & Waymouth, R. M. Catalysis as an enabling science for sustainable polymers. *Chem. Rev.* **118**, 839–885 (2018).

23. Coates, G. W. & Getzler, Y. D. Y. L. Chemical recycling to monomer for an ideal, circular polymer economy. *Nat. Rev. Mater.* **5**, 501–516 (2020).

24. Artz, J. et al. Sustainable conversion of carbon dioxide: an integrated review of catalysis and life cycle assessment. *Chem. Rev.* **118**, 434–504 (2018).

25. Deacy, A. C., Gregory, G. L., Sulley, G. S., Chen, T. T. D. & Williams, C. K. Sequence control from mixtures: switchable polymerization catalysis and future materials applications. *J. Am. Chem. Soc.* **143**, 10021–10040 (2021).

26. Zhu, Y., Romain, C. & Williams, C. K. Sustainable polymers from renewable resources. *Nature* **540**, 354–362 (2016).

27. Yu, Z. et al. A new route for the synthesis of propylene oxide from bio-glycerol derived propylene glycol. *Chem. Commun.* **14**, 3934–3936 (2009).

28. Shao, X. et al. Green production of phthalic anhydride from bio-based furan and maleic anhydride by an acid resin catalyst. *ACS Sustain. Chem. Eng.* **9**, 14385–14394 (2021).

29. Longo, J. M., Sanford, M. J. & Coates, G. W. Ring-opening copolymerization of epoxides and cyclic anhydrides with discrete metal complexes: structure–property relationships. *Chem. Rev.* **116**, 15167–15197 (2016).

30. Kremer, A. B. & Mehrkhodavandi, P. Dinuclear catalysts for the ring opening polymerization of lactide. *Coord. Chem. Rev.* **380**, 35–57 (2019).

31. Normand, M., Roisnel, T., Carpentier, J. F. & Kirillov, E. Dinuclear vs. mononuclear complexes: accelerated, metal-dependent ring-opening polymerization of lactide. *Chem. Commun.* **49**, 11692–11694 (2013).

32. Fortun, S., Daneshmand, P. & Schaper, F. Isotactic rac-lactide polymerization with copper complexes: the influence of complex nuclearity. *Angew. Chem. Int. Ed.* **54**, 13669–13672 (2015).

33. Santulli, F. et al. Bimetallic aluminum complexes bearing binaphthyl-based iminophenolate ligands as catalysts for the synthesis of polyesters. *Organometallics* **39**, 1213–1220 (2020).

34. Moore, D. R., Cheng, M., Lobkovsky, E. B. & Coates, G. W. Mechanism of the alternating copolymerization of epoxides and CO2 using β-diiminate zinc catalysts: evidence for a bimetallic epoxide enchainment. *J. Am. Chem. Soc.* **125**, 11911–11924 (2003).

35. Nakano, K., Hashimoto, S. & Nozaki, K. Bimetallic mechanism operating in the copolymerization of propylene oxide with carbon dioxide catalyzed by cobalt–salen complexes. *Chem. Sci.* **1**, 369–373 (2010).

36. Kissling, S. et al. Dinuclear zinc catalysts with unprecedented activities for the copolymerization of cyclohexene oxide and CO2. *Chem. Commun.* **51**, 4579–4582 (2015).

37. Nagae, H. et al. Lanthanide complexes supported by a trizinc crown ether as catalysts for alternating copolymerization of epoxide and CO2: telomerization controlled by carboxylate anions. *Angew. Chem. Int. Ed.* **57**, 2492–2496 (2018).

38. Asaba, H. et al. Alternating copolymerization of CO_2 and cyclohexene oxide catalyzed by cobalt–lanthanide mixed multinuclear complexes. *Inorg. Chem.* **59**, 7928–7933 (2020).

39. Li, J., Liu, Y., Ren, W.-M. & Lu, X.-B. Asymmetric alternating copolymerization of meso-epoxides and cyclic anhydrides: efficient access to enantiopure polyesters. *J. Am. Chem. Soc.* **138**, 11493–11496 (2016).

40. Liu, Y., Ren, W.-M., Zhang, W.-P., Zhao, R.-R. & Lu, X.-B. Crystalline CO2-based polycarbonates prepared from racemic catalyst through intramolecularly interlocked assembly. *Nat. Commun.* **6**, 8594 (2015).

41. Nakano, K., Hiyama, T. & Nozaki, K. Asymmetric amplification in asymmetric alternating copolymerization of cyclohexene oxide and carbon dioxide. *Chem. Commun.* **14**, 1871–1873 (2005).

42. Cui, L., Ren, B.-H. & Lu, X.-B. Trinuclear salphen–chromium(III) chloride complexes as catalysts for the alternating copolymerization of epoxides and cyclic anhydrides. *J. Polym. Sci.* **59**, 1821–1828 (2021).

43. Shi, Z., Jiang, Q., Song, Z., Wang, Z. & Gao, C. Dinuclear iron(iii) complexes bearing phenylene-bridged bis(amino triphenolate) ligands as catalysts for the copolymerization of cyclohexene oxide with carbon dioxide or phthalic anhydride. *Polym. Chem.* **9**, 4733–4743 (2018).

44. Diment, W. T. et al. Catalytic synergy using Al(III) and group 1 metals to accelerate epoxide and anhydride ring-opening copolymerizations. *ACS Catal.* **11**, 12532–12542 (2021).

45. Chamberlain, B. M. et al. Polymerization of lactide with zinc and magnesium β-diiminate complexes: stereocontrol and mechanism. *J. Am. Chem. Soc.* **123**, 3229–3238 (2001).

46. Sulley, G. S. et al. Switchable catalysis improves the properties of CO_2-derived polymers: poly(cyclohexene carbonate-b-ε-decalactone-b-cyclohexene carbonate) adhesives, elastomers, and toughened plastics. *J. Am. Chem. Soc.* **142**, 4367–4378 (2020).

47. Yang, G.-W., Zhang, Y.-Y. & Wu, G.-P. Modular organoboron catalysts enable transformations with unprecedented reactivity. *Acc. Chem. Res.* **54**, 4434–4448 (2021).

48. Aida, T., Sanuki, K. & Inoue, S. Well-controlled polymerization by metalloporphyrin. Synthesis of copolymer with alternating sequence and regulated molecular weight from cyclic acid anhydride and epoxide catalyzed by the system of aluminum porphyrin coupled with quaternary organic salt. *Macromolecules* **18**, 1049–1055 (1985).

49. Deacy, A. C., Kilpatrick, A. F. R., Regoutz, A. & Williams, C. K. Understanding metal synergy in heterodinuclear catalysts for the copolymerization of CO_2 and epoxides. *Nat. Chem.* **12**, 372–380 (2020).

50. Deacy, A. C., Moreby, E., Phanopoulos, A. & Williams, C. K. Co(III)/Alkali-Metal(I) heterodinuclear catalysts for the ring-opening copolymerization of CO_2 and propylene oxide. *J. Am. Chem. Soc.* **142**, 19150–19160 (2020).

51. Deacy, A. C., Phanopoulos, A., Lindeboom, W., Buchard, A. & Williams, C. K. Insights into the mechanism of carbon dioxide and propylene oxide ring-opening copolymerization using a Co(III)/K(I) heterodinuclear catalyst. *J. Am. Chem. Soc.* **144**, 17929–17938 (2022).

52. Reis, N. V., Deacy, A. C., Rosetto, G., Durr, C. B. & Williams, C. K. Heterodinuclear Mg(II)M(II) (M=Cr, Mn, Fe, Co, Ni, Cu and Zn) complexes for the ring opening copolymerization of carbon dioxide/epoxide and anhydride/epoxide. *Chem. Eur. J.* **28**, e202104198 (2022).

53. Lindeboom, W., Fraser, D. A. X., Durr, C. B. & Williams, C. K. Heterodinuclear Zn(II), Mg(II) or Co(III) with Na(I) catalysts for carbon dioxide and cyclohexene oxide ring opening copolymerizations. *Chem. Eur. J.* **27**, 12224–12231 (2021).

54. Garden, J. A., Saini, P. K. & Williams, C. K. Greater than the sum of its parts: a heterodinuclear polymerization catalyst. *J. Am. Chem. Soc.* **137**, 15078–15081 (2015).

55. Deacy, A. C., Durr, C. B., Kerr, R. W. F. & Williams, C. K. Heterodinuclear catalysts Zn(II)/M and Mg(II)/M, where M = Na(I), Ca(II) or Cd(II), for phthalic anhydride/cyclohexene oxide ring opening copolymerisation. *Catal. Sci. Technol.* **11**, 3109–3118 (2021).

56. Chen, H.-Y., Mialon, L., Abboud, K. A. & Miller, S. A. Comparative study of lactide polymerization with lithium, sodium, magnesium, and calcium complexes of BHT. *Organometallics* **31**, 5252–5261 (2012).

57. Gao, B. et al. Stereoselective ring-opening polymerization of rac-lactides catalyzed by aluminum hemi-salen complexes. *Organometallics* **32**, 5435–5444 (2013).

58. Dai, Z. et al. Simple sodium and potassium phenolates as catalysts for highly isoselective polymerization of rac-lactide. *Catal. Sci. Technol.* **6**, 515–520 (2016).

59. Lidston, C. A. L., Abel, B. A. & Coates, G. W. Bifunctional catalysis prevents inhibition in reversible-deactivation ring-opening copolymerizations of epoxides and cyclic anhydrides. *J. Am. Chem. Soc.* **142**, 20161–20169 (2020).

60. Darensbourg, D. J. Chain transfer agents utilized in epoxide and CO_2 copolymerization processes. *Green. Chem.* **21**, 2214–2223 (2019).

61. Izatt, R. M. et al. Calorimetric titration study of the interaction of several uni- and bivalent cations with 15-crown-5, 18-crown-6, and two isomers of dicyclohexo-18-crown-6 in aqueous solution at 25 °C and μ = 0.1. *J. Am. Chem. Soc.* **98**, 7620–7626 (1976).

62. Paul, S. et al. Ring-opening copolymerization (ROCOP): synthesis and properties of polyesters and polycarbonates. *Chem. Commun.* **51**, 6459–6479 (2015).

63. Inkinen, S., Hakkarainen, M., Albertsson, A.-C. & Södergård, A. From lactic acid to poly(lactic acid) (PLA): characterization and analysis of PLA and its precursors. *Biomacromolecules* **12**, 523–532 (2011).

64. Shannon, R. D. Revised effective ionic radii and systematic studies of interatomic distances in halides and chalcogenides. *Acta Cryst. A* **32**, 751–767 (1976).

65. Kumar, A. & Blakemore, J. D. On the use of aqueous metal-aqua pK_a values as a descriptor of lewis acidity. *Inorg. Chem.* **60**, 1107–1115 (2021).

66. Abel, B. A., Lidston, C. A. L. & Coates, G. W. Mechanism-inspired design of bifunctional catalysts for the alternating ring-opening copolymerization of epoxides and cyclic anhydrides. *J. Am. Chem. Soc.* **141**, 12760–12769 (2019).

67. Wang, X.-x et al. The comparison of pK_a determination between carbonic acid and formic acid and its application to prediction of the hydration numbers. *Chem. Phys. Lett.* **460**, 339–342 (2008).

68. Karasawa, T., Kumagai, N. & Shibasaki, M. Heterogeneous hetero-bimetallic catalysis enabling expeditious access to CF3-containing vic-amino alcohols. *Org. Lett.* **20**, 308–311 (2018).

69. Karasawa, T., Oriez, R., Kumagai, N. & Shibasaki, M. anti-selective catalytic asymmetric nitroaldol reaction of α-keto esters: intriguing solvent effect, flow reaction, and synthesis of active pharmaceutical ingredients. *J. Am. Chem. Soc.* **140**, 12290–12295 (2018).

70. Wu, R., Wang, S., Zhou, N., Cao, Z. & Zhang, Y. A proton-shuttle reaction mechanism for histone deacetylase 8 and the catalytic role of metal ions. *J. Am. Chem. Soc.* **132**, 9471–9479 (2010).

71. Wang, L. et al. Kinetic analysis of the living ring-opening polymerisation of L-Lactide with tin(II) initiators. *Eur. J. Inorg. Chem.* **2013**, 5896–5905 (2013).

72. Kowalski, A., Duda, A. & Penczek, S. Polymerization of l,l-Lactide initiated by aluminum isopropoxide trimer or tetramer. *Macromolecules* **31**, 2114–2122 (1998).

Acknowledgements

Author contributions

F.F., W.D. and A.D. conceived and conducted all experiments; F.F. and R.K. performed all crystallographic characterization. C.W. and S.F. conceived the project, led the research team, and secured the research funding.

Competing interests

C.W. is a director of Econic Technologies. The other authors declare no competing interests.

Additional information

Supplementary information The online version contains supplementary material available at https://doi.org/10.1038/s41467-023-40284-z.

Correspondence and requests for materials should be addressed to Charlotte K. Williams.

Peer review information *Nature Communications* thanks Donald Darensbourg and Bun Yeoul Lee for their contribution to the peer review of this work. A peer review file is available.

Reprints and permissions information is available at http://www.nature.com/reprints

Publisher's note Springer Nature remains neutral with regard to jurisdictional claims in published maps and institutional affiliations.